Zirconium(IV) Sandwich Complexes of Porphyrins and Tetraazaporphyrins: Synthesis, Structure, and Nonlinear Optical Properties

James P. Collman,* Jonathan L. Kendall, Judy L. Chen, and Todd A. Eberspacher

Department of Chemistry, Stanford University, Stanford, California 94305

Christopher R. Moylan*

IBM Almaden Research Center, 650 Harry Road, San Jose, California 95120

Received May 30, 1997[⊗]

A family of bis(porphyrin) zirconium sandwich complexes containing octaethylporphyrin (OEP) and octaethyltetraazaporphyrin (OETAP) was synthesized and characterized by UV−vis and NMR spectroscopies. The two ligands are structural analogues yet have dramatically different redox properties (the redox potentials of OETAP complexes are much more positive than those of the corresponding OEP complexes). Cyclic voltammetry results indicate that $Zr(OETAP)_2$ is about 600 mV harder to oxidize and about 600 mV easier to reduce than $Zr(OEP)_2$, while the mixed sandwich Zr(OEP)(OETAP) exhibits intermediate redox potentials. The structures of Zr(OEP)(OETAP) and $Zr(OETAP)_2$ were determined by X-ray crystallography and compared to $Zr(OEP)_2$. The solid-state structures were very similar, indicating that OEP and OETAP have similar steric parameters and that observed spectroscopic and electrochemical differences are due primarily to electronic factors. The one electron oxidized porphyrin sandwiches were also synthesized. Characterization by UV−vis, near-IR, EPR, and IR spectroscopies confirm the π radical nature of these complexes. IR spectra indicate that the cation is delocalized over the entire complex in both $[Zr(OEP)(OETAP)]^+[SbCl_6]^-$ and $[Zr(OETAP)_2]^+[SbCl_6]^-$, consistent with a strongly coupled π system. Additional evidence for strong coupling was obtained from measurement of the nonlinear optical properties of the mixed complex; the molecular hyperpolarizability is negative, indicating that the dipole moment reverses direction upon electronic excitation.

Introduction

The unique properties of porphyrin sandwich complexes (compounds with a large metal ion "sandwiched" between two porphyrin ligands and having the general formula M(porphyrin)$_2$) stem from strong interactions between the two macrocycles. Porphyrin sandwich complexes have been studied as models for the "special pair" in the photosynthetic reaction center of bacteriorhodopsin.[1] The metal in a sandwich complex holds the porphyrins closer than their van der Waals distance, which results in strong $\pi-\pi$ interactions between the macrocycles and a splitting of the local porphyrin HOMOs into porphyrin−porphyrin bonding and antibonding orbitals. For a given macrocycle, the closer the ligands are held together the stronger the interactions. These effects are most pronounced in zirconium(IV) sandwiches, as zirconium(IV) is one of the smallest metal ions known to form porphyrin sandwiches.

Complexes in which the two macrocycles are the same[2−16] (homo-sandwiches) and different[15−24] (mixed-sandwiches) have been synthesized. Previously reported mixed sandwiches have been prepared using ligands having a great deal of structural variation but little electronic variation: octaethylporphyrin (OEP), tetraphenylporphyrin (TPP), and phthalocyanine (Pc) are very different structurally, but the redox potentials of Pc and TPP complexes are only 150−250 mV more positive than those of OEP complexes.[25]

[⊗] Abstract published in *Advance ACS Abstracts,* October 15, 1997.

(1) Girolami, G. S.; Hein, C. L.; Suslick, K. S. *Angew. Chem., Int. Ed. Engl.* **1996**, *35*, 1223−1225.
(2) Kim, K.; Lee, W. S.; Kim, H.-J.; Cho, S.-H.; Girolami, G. S.; Gorlin, P. A.; Suslick, K. S. *Inorg. Chem.* **1991**, *30*, 2652−2656.
(3) Buchler, J. W.; De Cian, A.; Elschner, S.; Fischer, J.; Hammerschmitt, P.; Weiss, R. *Chem. Ber.* **1992**, *125*, 107−115.
(4) Buchler, J. W.; De Cian, A.; Fischer, J.; Hammerschmitt, P.; Weiss, R. *Chem. Ber.* **1991**, *124*, 1051−1058.
(5) Buchler, J. W.; De Cian, A.; Fischer, J.; Kiln-Botulinski, M; Paulus, H.; Weiss, R. *J. Am. Chem. Soc.* **1986**, *108*, 3652−3659.
(6) Buchler, J. W.; Elsässer, K.; Kihn-Botulinski, M.; Scharbert, B. *Angew. Chem., Int. Ed. Engl.* **1986**, *25*, 286−287.
(7) Kim, H.-J.; Whang, D.; Kim, J.; Kim, K. *Inorg. Chem.* **1992**, *31*, 3882−3886.
(8) Girolami, G. S.; Milam, S. N.; Suslick, K. S. *Inorg. Chem.* **1987**, *26*, 343−344.
(9) Girolami, G. S.; Milam, S. N.; Suslick, K. S. *J. Am. Chem. Soc.* **1988**, *110*, 2011−2012.
(10) Buchler, J. W.; Hüttermann, J.; Löffler, *J. Bull. Chem. Soc. Jpn.* **1988**, *61*, 71−77.
(11) Buchler, J. W.; Kihn-Botulinski, M.; Löffler, J.; Scharbert, B. *New J. Chem.* **1992**, *16*, 545−553.
(12) Buchler, J. W.; De Cian, A.; Fischer, J.; Kihn-Botulinski, M.; Weiss, R. *Inorg. Chem.* **1988**, *27*, 339−345.
(13) Bucher, J. W.; Scharbert, B. *J. Am. Chem. Soc.* **1988**, *110*, 4272−4276.
(14) De Cian, A.; Moussavi, M.; Fischer, J.; Weiss, R. *Inorg. Chem.* **1985**, *24*, 3162−3167.
(15) Buchler, J. W.; De Cian, A.; Fischer, J.; Hammerschmitt, P.; Löffler, J.; Scharbert, B.; Weiss, R. *Chem. Ber.* **1989**, *122*, 2219−2228.
(16) Kadish, K. M.; Moninot, G.; Hu, Y.; Dubois, D.; Ibnlfassi, A.; Barbe, J.-M.; Guilard, R. *J. Am. Chem. Soc.* **1993**, *115*, 8153−8166.
(17) Girolami, G. S.; Gorlin, P. A.; Suslick, K. S. *Inorg. Chem.* **1994**, *33*, 626−627.
(18) Guilard, R.; Barbe, J.-M.; Ibnlfassi, A.; Zrineh, A.; Adamian, V. A.; Kadish, K. M. *Inorg. Chem.* **1995**, *34*, 1472−1481.
(19) Lachkar, M.; De Cian, A.; Fischer, J.; Weiss, R. *New J. Chem.* **1988**, *12*, 729−731.
(20) Bilsel, O.; Rodriguez, J.; Milam, S. N.; Gorlin, P. A.; Girolami, G. S.; Suslick, K. S.; Holten, D. *J. Am. Chem. Soc.* **1992**, *114*, 6528−6538.
(21) Chabach, D.; Tahiri, M.; De Cian, A.; Fischer, J.; Weiss, R.; El Malouli Bibout, M. *J. Am. Chem. Soc.* **1995**, *117*, 8548−8556.
(22) Spyroulias, G. A.; Coutsolelos, A. G.; Raptopoulou, C. P.; Terzis, A. *Inorg. Chem.* **1995**, *34*, 2476−2479.
(23) Spyroulias, G. A.; Coutsolelos, A. G. *Inorg. Chem.* **1996**, *35*, 1382−1385.
(24) Buchler, J. W.; Löffler, J. *Z. Naturforsch* **1990**, *45b*, 531−542.

S0020-1669(97)00657-5 CCC: $14.00

The purpose of the present work is to study the properties of a family of zirconium(IV) sandwich complexes containing porphyrin ligands that are structurally similar but electrochemically quite different: OEP and octaethyltetraazaporphyrin (OETAP). The structure of OETAP is very similar to OEP with the exception that nitrogens are substituted for the four methine groups. However, the redox potentials of OETAP complexes are ca 0.5 V more positive than those of the corresponding OEP complexes.[26] The complete family of $Zr(OEP)_2$, Zr(OEP)(OETAP), and $Zr(OETAP)_2$ allows the study of electronic effects on the physical properties of porphyrin sandwiches without a conspicuous change in steric parameters. We present here the synthesis and characterization of Zr(OEP)(OETAP), $Zr(OETAP)_2$, and the one-electron oxidized species, $[Zr(OEP)(OETAP)]^+[SbCl_6]^-$ and $[Zr(OETAP)_2]^+[SbCl_6]^-$. These complexes are compared with the known members of the family: $Zr(OEP)_2$ and $[Zr(OEP)_2]^+[SbCl_6]^-$.[3]

Since mixed porphyrin sandwich complexes are noncentrosymmetric and have two large π systems that show strong $\pi-\pi$ interactions, they are attractive molecules for second-order nonlinear optical studies and have potential as nonlinear optical materials.[17] However, nonlinear optical properties of such sandwich complexes have not been reported. We report here the second-order nonlinear optical properties of a mixed porphyrin sandwich, Zr(OEP)(OETAP). The large difference in porphyrin electronegativities makes this compound a good candidate for second-order nonlinear optical studies.

Experimental Section

Reagents and Solvents. All solvents and chemicals were of reagent grade and were used as received except as indicated below. Toluene and ethylene glycol dimethyl ether (DME) were distilled from potassium−benzophenone ketyl and sodium−potassium−benzophenone ketyl, respectively. Dichloromethane was distilled from phosphorus pentoxide. Tetrahydrofuran (THF) was vacuum transferred from sodium−benzophenone ketyl immediately prior to use. Tetrabutylammonium hexafluorophosphate was recrystallized from ethanol. $Zr(OEP)_2$,[2] $Zr(OEP)(Cl)_2$,[27] H_2OETAP,[28] $Zr(NEt_2)_4$,[29] Zn(OEP),[30] and tris(4-bromophenyl)aminium hexachloroantimonate[31] were synthesized according to literature procedures.

Physical Methods. All manipulations of oxygen- and water-sensitive materials were performed in a nitrogen-filled Vacuum Atmosphere Co. dry box or in Schlenkware under an argon atmosphere. Oxygen levels in the dry box were monitored with an AO 316-C trace oxygen analyzer and were maintained below 1 ppm. ^{1}H NMR spectra were obtained on a Nicolet NMC WB-300 300-MHz spectrometer. UV−vis spectra were recorded on a Hewlett Packard 8453 diode array spectrophotometer. IR spectra were obtained on a Mattson Infinity 60AR FTIR. EPR spectra were recorded on a Bruker ER 220-D-SRC spectrometer; sample temperatures were maintained at 77 K using a liquid-nitrogen-cooled finger dewar. Mass spectra and elemental analyses were performed by the Mass Spectrometry Facility of the University of California at San Francisco and by Midwest Microlab, respectively.

Electrochemical studies were performed on an EG&G Princeton Applied Research Model 273A potentiostat/galvanostat. The cyclic voltammetry cell consisted of platinum working and counter electrodes and a silver wire as a reference electrode. The sample concentrations were 5×10^{-4} M. The supporting electrolyte was NBu_4PF_6 (0.2 M). Ferrocene was used as an internal standard.

Electric field-induced second harmonic (EFISH) generation experiments and dipole moment measurements on Zr(OEP)(OETAP) were performed in chloroform solution at 1907 nm as previously described.[32] The B convention of Willetts *et al.*[33] was used to define hyperpolarizability. The second harmonic measurements were calibrated against a quartz crystal, using the currently recommended value[34] of the nonlinearity of quartz (6.7×10^{-10} esu).

Syntheses. $Li_2(OETAP)(DME)_2$. $Li_2(OETAP)(DME)_2$ was synthesized by a procedure similar to that of the OEP adduct.[35] In a nitrogen-filled dry box, 1.05 g (1.95 mmol) of H_2OETAP, 0.737 g (4.4 mmol) of lithium bis(trimethylsilyl)amide, and DME (50 mL) were added to a 100 mL round bottom flask. The reaction mixture was heated at reflux for 8 h. The reaction was cooled to room temperature, and the solvent was reduced in volume under vacuum to 10 mL. Hexane (10 mL) was added to the reaction flask, which was then heated at reflux to dissolve the solid. The solution was slowly cooled to 0 °C and allowed to sit overnight at 0 °C. The mixture was filtered, leaving a blue crystalline product. The crystals were washed with 5 mL of DME and then dried at 10^{-3} Torr for 0.5 h yielding 1.09 g (1.49 mmol) of product (77% yield). ^{1}H NMR (acetone-d_6): δ 3.87 (q, 16 H, $-CH_2-$), 3.44 (s, 8 H, $-OCH_2-$), 3.26 (s, 12 H, $-OCH_3$), 1.82 (t, 24 H, $-CH_3$). UV−vis (DME): λ_{max} 339 (Soret), 554, 601 nm.

Zr(OEP)(OETAP). In the nitrogen dry box, 837 mg (1.20 mmol) of $Zr(OEP)(Cl)_2$ and 493 mg (1.92 mmol) of silver triflate were dissolved in 100 mL of toluene. The solution was heated at 80 °C for 10 h. The reaction was cooled to room temperature and 1.00 g (1.37 mmol) of $Li_2(OETAP)(DME)_2$ was added to the solution. The solution was heated at reflux for 36 h. The solvent was removed under vacuum; the black residue was extracted into hexanes and filtered. The filtrate was separated on an alumina column using a gradient of hexane to 3:1 hexane/toluene as the eluent. The product was collected as the first green band. The solvent was removed under vacuum yielding 1.027 g (0.885 mmol) of product (74% yield). ^{1}H NMR (C_6D_6): δ 9.60 (s, 4 H, meso H), 4.23 (m, 8 H, $-CH_2-$), 4.09 (m, 8 H, $-CH_2-$), 3.87 (m, 8 H, $-CH_2-$), 3.63 (m, 8 H, $-CH_2-$), 1.64 (t, 24 H, $-CH_3$), 1.55 (t, 24 H, $-CH_3$). UV−vis (CH_2Cl_2) λ_{max} (log ϵ) 336 (Soret) (5.00), 378 (Soret) (4.81), 430 (4.49), 520 (sh), 550 (4.22), 598 (4.49), 922 (3.18) nm. MS *m/e* 1159.7 (MH^+). IR (KBr, cm^{-1}): 2963 (s), 2930 (s), 2870 (s), 1494 (m), 1463 (s), 1452 (m), 1399 (m), 1366 (s), 1261 (m), 1150 (m), 1142 (m), 1110 (w), 1064 (m), 1057 (m), 1015 (s), 983 (m), 953 (s), 914 (m), 843 (m), 796 (w), 770 (w), 746 (w), 702 (w), 687 (w). Anal. Calc for $C_{68}H_{84}N_{12}Zr$: C, 70.37; H, 7.29; N, 14.48. Found: C, 70.24; H, 7.36; N, 14.46.

$Zr(OETAP)_2$. In the dry box, 172 mg (0.320 mmol) of H_2OETAP was dissolved in 13 mL of toluene. The solution was heated at reflux, and 63 mg (0.166 mmol) $Zr(NEt_2)_4$ was added to the solution. After 48 h the solvent was removed under vacuum. The residual solid was purified on a silica column using 90% hexane/10% toluene as an eluent. The product was collected as the first purple band. The solvent was removed under vacuum yielding 114 mg (0.0979 mmol) of product (61% yield). ^{1}H NMR (C_6D_6): δ 4.19 (m, 16 H, $-CH_2-$), 3.71 (m, 16 H, $-CH_2-$), 1.66 (t, 48 H, $-CH_3$). UV−vis (CH_2Cl_2) λ_{max} (log ϵ) 332 (Soret) (5.03), 546 (4.58), 620 (4.67), 850 (2.87) nm. MS: *m/e* 1163.6 (MH^+). IR (KBr, cm^{-1}): 2964 (s), 2932 (s), 2871 (s), 1488 (m), 1461 (s), 1442 (m), 1379 (s), 1260 (m), 1151 (m), 1013 (s), 954 (s), 914 (m), 799 (w), 771 (w), 745 (w), 706 (w). Anal. Calc for $C_{64}H_{80}N_{16}Zr$: C, 66.00; H, 6.92; N, 19.25. Found: C, 66.51; H, 7.09; N, 18.70.

$[Zr(OEP)(OETAP)]^+[SbCl_6]^-$. A solution of 13 mg (11 mmol) of Zr(OEP)(OETAP) in 1 mL of dichloromethane was placed into a 20 mL vial. A solution of 9.1 mg (11 mmol) of tris(4-bromophenyl)-

(25) Kadish, K. M. *Prog. Inorg. Chem.* **1986**, *34*, 435−605.
(26) Fitzgerald, J. P.; Haggerty, B. S.; Rheingold, A. L.; May, L.; Brewer, G. A. *Inorg. Chem.* **1992**, *31*, 2006−2013.
(27) Brand, H.; Arnold, J. *Organometallics* **1993**, *12*, 3655−3665.
(28) Fitzgerald, J.; Taylor, W.; Owen, H. *Synthesis* **1991**, 686.
(29) (a) Bradly, D. C.; Thomas, I. M. *J. Chem. Soc.* **1960**, 3857−3861. (b) Chandra, G.; Lappert, M. F. *J. Chem. Soc. A* **1968**, 1940−1945.
(30) Buchler, J. W. In *Porphyrins and Metalloporphyrins*; Smith, K. M., Ed.; Elsevier: Amsterdam, 1975; Chapter 5.
(31) Bell, F. A.; Ledwith, A.; Sherrington, D. C. *J. Chem. Soc. C* **1969**, 2719−2720.
(32) Moylan, C. R.; Miller, R. D.; Twieg, R. J.; Betterton, K. M.; Lee, V. Y.; Matray, T. J.; Nguyen, C. *Chem. Mater.* **1993**, *5*, 1499−1508.
(33) Willetts, A.; Rice, J. E.; Burland, D. M.; Shelton, D. P. *J. Chem. Phys.* **1992**, *97*, 7590−7599.
(34) Moylan, C. R.; Miller, R. D.; Twieg, R. J.; Lee, V. Y. In *Polymers for Second-Order Nonlinear Optics*; ACS Symp. Ser. Vol. 601; American Chemical Society: Washington, DC, 1995; Chapter 5.
(35) Arnold, J.; Dawson, D. Y.; Hoffman, C. G. *J. Am. Chem. Soc.* **1993**, *115*, 2707−2713.

aminium hexachloroantimonate in 2 mL of dichloromethane was added to the reaction vial and stirred 5 min. The product was precipitated by slow diffusion of pentane into the dichloromethane layer. The precipitate was collected on a glass frit and dried under vacuum leaving 17 mg (11 mmol) of product (100% yield). UV−vis (CH_2Cl_2) λ_{max} (log ϵ) 331 (Soret) (5.08), 451 (4.38), 560 (4.23), 640 (3.40), 717 (3.64) nm. Near-IR (CH_2Cl_2): λ_{max} (log ϵ) 999 (4.04), 1106 (4.00). IR (KBr, cm^{-1}): 2970 (s), 2934 (s), 2873 (s), 1547 (m), 1464 (m), 1420 (w), 1376 (w), 1338 (w), 1317 (w), 1263 (w), 1138 (w), 1129 (m), 1101 (w), 1055 (s), 1016 (s), 982 (w), 955 (s), 800 (w), 775 (w), 745 (w), 715 (w). EPR (77 K, CH_2Cl_2): $g = 2.005$.

$[Zr(OETAP)_2]^+[SbCl_6]^-$. A solution of 11 mg (9.4 mmol) of $Zr(OETAP)_2$ in 1 mL of dichloromethane was placed in a 20 mL vial. A solution of 7.7 mg (9.4 mmol) of tris(4-bromophenyl)aminium hexachloroantimonate in 3 mL of dichloromethane was added to the reaction vial; the reaction was stirred for 5 min. The product was crystallized by slow diffusion of pentane into the dichloromethane layer. The crystals were collected on a glass frit and dried under vacuum leaving 10.3 mg (6.9 mmol) of product (73% yield). UV−vis (CH_2Cl_2): λ_{max} (log ϵ) 266 (4.58), 324 (Soret) (5.17), 499 (3.78), 538 (4.02), 581 (4.86), 708 (3.35), 795 (3.75). Near-IR (CH_2Cl_2) λ_{max} (log ϵ) 1096 (4.00), 1209 (4.14), ∼1280 (3.93) (inflection) nm. IR (KBr, cm^{-1}): 2970 (s), 2935 (s), 2872 (s), 1464 (m), 1457 (m), 1418 (m), 1371 (m), 1353 (w), 1321 (m), 1290 (w), 1261 (m), 1153 (w), 1133 (m), 1056 (s), 1020 (s), 979 (w), 955 (s), 800 (w), 775 (s), 744 (w), 714 (w). EPR (77 K, CH_2Cl_2): $g = 2.005$. Anal. Calc for $C_{64}H_{80}Cl_6N_{16}SbZr$: C, 51.28; H, 5.38; N, 14.95. Found: C, 51.49; H, 5.58; N, 14.09.

Zn(OETAP). To a 250 mL round bottom flask were added solutions of 44 mg (0.0818 mmol) of H_2OETAP in 30 mL of dichloromethane and 50 mg (0.228 mmol) of zinc acetate dihydrate in 4 mL of methanol. The reaction was heated at reflux for 1 h. The reaction was cooled to room temperature, and the product was separated on a silica column using dichloromethane as the eluent. The first band (purple) was unreacted H_2OETAP. The second band (blue) was eluted with 98% dichloromethane/2% methanol and was collected as the product. The solvent was removed under vacuum yielding 39 mg (0.065 mmol) of product (79% yield). UV−vis (CH_2Cl_2): λ_{max} (log ϵ) 341 (5.02), 544 (4.25), 593 (5.10) nm. ^1H NMR ($CDCl_3$): δ 3.93 (q, 16 H, $-CH_2-$), 1.83 (t, 24 H, $-CH_3$). IR (KBr, cm^{-1}): 2972 (s), 2962 (s), 2932 (s), 2870 (s), 1472 (m), 1458 (s), 1374 (m), 1264 (m), 1151 (m), 1104 (w), 1067 (w), 1055 (w), 1013 (s), 957 (s), 907 (w), 763 (s), 744 (s).

$[Zn(OETAP)]^+[SbCl_6]^-$. In the nitrogen box, a 20 mL vial was charged with 12.6 mg (0.0209 mmol) of Zn(OETAP), 17.0 mg (0.0209 mmol) of tris(4-bromophenyl)aminium hexachloroantimonate, and 2 mL of acetonitrile. The reaction was stirred for 5 min. The reaction solution was filtered, and the solvent was removed under vacuum. The product was precipitated with pentane from a dichloromethane solution. The product was not air stable in solution. UV−vis (CH_2Cl_2): λ_{max} 310 (Soret), 610, 635 nm. IR (KBr, cm^{-1}): 2967 (s), 2932 (s), 2871 (s), 1486 (s), 1461 (m), 1454 (m), 1384 (w), 1311 (s), 1284 (m), 1265 (m), 1145 (w), 1100 (w), 1068 (m), 1056 (m), 1007 (s), 985 (w), 955 (s), 820 (m), 733 (w).

X-ray Crystal Structure Determination of Zr(OEP)(OETAP) and $Zr(OETAP)_2$. Single crystals of the Zr(OEP)(OETAP) molecule are, at -60 ± 2 °C, monoclinic, space group $P2_1/n$ (an alternate setting of No. 14) with $a = 15.425(3)$ Å, $b = 15.265(3)$ Å, $c = 25.783(5)$ Å, $\beta = 92.43(3)°$, and $Z = 4$ {$d_{calcd} = 1.271$ g·cm^{-1}; μ(Mo Kα) = 0.23 mm^{-1}}. Single crystals of the $Zr(OETAP)_2$ molecule are, at -80 ± 2 °C, monoclinic, space group $P2_1/n$ (an alternate setting of No. 14) with $a = 15.405(3)$ Å, $b = 15.250(3)$ Å, $c = 25.600(5)$ Å, $\beta = 92.63(3)°$, and $Z = 4$ {$d_{calcd} = 1.228$ g·cm^{-1}; μ(Mo Kα) = 0.24 mm^{-1}}. Totals of 8229 [Zr(OEP)(OETAP)] and 28466 [$Zr(OETAP)_2$] independent reflections having 2θ(Mo Kα) < 43.8° or < 55° [the equivalent of 0.8 and 1.00 limiting Cu Kα spheres] were collected on a Nonius CADD 4 computer-controlled diffractometer [Zr(OEP)(OETAP)] or a Siemens SMART CCD autodiffractometer [$Zr(OETAP)_2$].

Both structures were solved using "heavy-atom" Patterson techniques with the Siemens SHELXTL-PC software package. The resulting structural parameters have been refined to convergence {R_1 (unweighted, based on F) = 0.041 and 0.040 for 6456 and 7254 independent reflections} using counter-weighted full-matrix least-squares techniques and structural models which incorporated anisotropic thermal parameters for all full-occupancy non-hydrogen atoms. Isotropic thermal parameters were used for one disordered (minor occupancy) methyl carbon C_{32b} in both Zr(OEP)(OETAP) and $Zr(OEP)_2$.

The individual prophyrin rings of Zr(OEP)(OETAP) could not be distinguished. This disorder was included in the structural model by using equal weight (50%, 50%) carbon and nitrogen atoms at equivalent positions with common thermal parameters for the meso atoms of the porphyrin macrocycles. Hydrogen atoms on the meso carbon atoms were included at 50% occupancy at all eight positions and refined as independent atoms with the thermal parameter fixed at 1.2 times the equivalent thermal parameter of the carbon to which it is attached. Additional cycles of least-squares refinement were conducted by allowing the carbon and nitrogen occupancies to vary and converged at 0.48(1)% C for ring "a" and 0.52(2)% C for ring "b" and were therefore included in all subsequent calculations as equal populations.

Table 1. UV−Vis−Near-IR Data for Porphyrin Sandwich Complexes and Their Cations in Dichloromethane Solution[a]

	Soret	Q bands	near-IR
$Zr(OEP)_2$	382[b]	490, 550, 592, 750	
Zr(OEP)(OETAP)	336, 378	430, 520, 550, 598, 922	
$Zr(OETAP)_2$	332	546, 620, 850	
$[Zr(OEP)_2]^+$	358	430, 508, 684	966
$[Zr(OEP)(OETAP)]^+$	331	451, 560, 640, 717	999, 1106
$[Zr(OETAP)_2]^+$	324	499, 538, 581, 708, 795	1096, 1209

[a] All values are in nm. Data for $Zr(OEP)_2$ and $[Zr(OEP)_2]^+$ are from refs 2 and 3. [b] $Zr(OEP)_2$ also showed a shoulder at 355 nm.

Results and Discussion

Synthesis. The synthesis of $Zr(OETAP)_2$ was a straightforward adaptation of Kim's $Zr(OEP)_2$ synthesis[2] but gave a slightly higher yield. $Zr(NEt_2)_4$ was allowed to react with H_2OETAP in refluxing toluene, giving a 61% yield of $Zr(OETAP)_2$.

Zr(OEP)(OETAP) was obtained in high yield from $Zr(OEP)(OTf)_2$ and $Li_2OETAP(DME)_2$. $Zr(OEP)(Cl)_2$ was synthesized according to the method published by Arnold.[27] The dichloride species was converted to the ditriflate adduct and then was combined with $Li_2(OETAP)(DME)_2$ at reflux in toluene. Neither of the two corresponding homo-sandwiches were observed from this reaction.

Direct reaction of the dichloride species with $Li_2(OETAP)(DME)_2$ in toluene did not form the mixed porphyrin sandwich. The desired product was obtained via the direct reaction method using higher boiling solvents, but lower yields and greater decomposition of starting materials resulted. For example, only a 5% yield of Zr(OEP)(OETAP) was obtained when the reaction was heated at reflux in 1-chloronaphthalene (bp 260 °C).

The oxidized species were obtained from the reaction of the oxidant tris(4-bromophenyl)aminium hexachloroantimonate with the neutral compounds and then isolated by crystallization or precipitation of the product. $[Zr(OEP)(OETAP)]^+[SbCl_6]^-$ is stable in solution, but $[Zr(OETAP)_2]^+[SbCl_6]^-$ is reduced to the neutral species in solution when exposed to the atmosphere for several days.

UV−Vis−Near-IR. The electronic spectra of these sandwiches are given in Table 1, where they are compared to the results previously obtained for $Zr(OEP)_2$ and $[Zr(OEP)_2]^+$.[2,3]

Both neutral compounds show spectra indicative of sandwich complexes. $Zr(OETAP)_2$ has a Soret band at 332 nm, which is blue-shifted by 8 nm with respect to the corresponding monoporphyrin.[28] The blue shift is consistent with strong $\pi-\pi$ interactions and has been observed in other porphyrin sandwich complexes and cofacial porphyrin complexes.[5,36] The spectrum

(36) Bilsel, O.; Rodriguez, J.; Milam, S. N.; Gorlin, P. A.; Girolami, G. S.; Suslick, K. S.; Holten, D. *J. Am. Chem. Soc.* **1992**, *114*, 6528−6538.

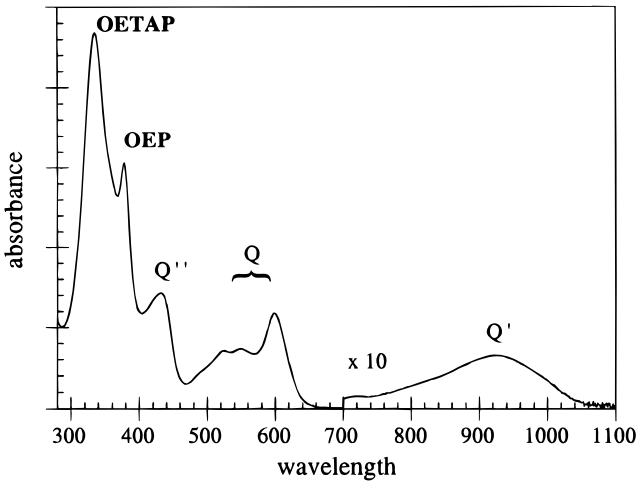

Figure 1. UV−vis spectrum of Zr(OEP)(OETAP) in dichloromethane.

Table 2. Half-Wave Potentials for Porphyrin Sandwich Complexes in THF[a]

	$E_{1/2}$(ox2)	$E_{1/2}$(ox1)	$E_{1/2}$(red1)	$E_{1/2}$(red2)	$E_{1/2}$(red3)
$Zr(OEP)_2$	+0.66	+0.21	−1.45	−1.76	
Zr(OEP)(OETAP)	+0.96	+0.48	−1.04	−1.44	−2.20
$Zr(OETAP)_2$		+0.80	−0.82	−1.21	−1.86

[a] All values are in V and are reported *vs* Ag/AgCl using $Cp_2Fe^{III/II}$ (0.56 V *vs* Ag/AgCl; see ref 42) as an internal standard. Data were collected using a Pt working electrode, Pt counter electrode, and Ag/AgCl reference electrode. Tetrabutylammonium hexafluorophosphate was used as a supporting electrolyte.

of Zr(OEP)(OETAP), Figure 1, shows two Soret bands, the identities of which can be assigned on the basis of the Soret bands in the corresponding homo-sandwiches; the band at 336 nm corresponds to the OETAP subunit, and the band at 378 nm corresponds to the OEP subunit.

Another characteristic of sandwich complexes is the appearance of absorption bands shifted to the red (termed Q′) and to the blue (termed Q″) of the normal Q band region of monoporphyrins. The new transitions are thought to result from orbitals delocalized over the two porphyrins.[36] All of the neutral sandwiches in Table 2 show the Q′ and Q″ bands indicative of a strongly coupled system. The band at 546 nm in the $Zr(OETAP)_2$ complex is tentatively assigned as the Q″ band, although it is in the Q band region for tetraazaporphyrins.

The UV−vis/near-IR data for the monocations are presented in Table 1. For $[Zr(OETAP)_2]^+[SbCl_6]^-$ the Soret is blue shifted by 8 nm, indicating stronger $\pi-\pi$ interactions, which is not surprising since oxidation of the sandwich involves removal of an electron from the $\pi-\pi$ antibonding orbital. In $[Zr(OEP)(OETAP)]^+[SbCl_6]^-$ only one Soret appears at 331 nm, which is similar but slightly blue-shifted compared to the OETAP Soret in the neutral complex. Since the Soret corresponding to the more electron-rich OEP ligand is no longer present, it is likely that the electron has been removed from an orbital which is mostly OEP in character. A shoulder appearing at 355 nm may be associated with the OEP subunit.

A characteristic of porphyrin sandwich radical cations is a moderately intense, broad absorption in the near-IR region. This near-IR band has been attributed to the porphyrin−porphyrin bonding to antibonding transition. $[Zr(OEP)(OETAP)]^+[SbCl_6]^-$ shows two maxima at 999 and 1106 nm, with the higher energy band having a slightly larger extinction coefficient. $[Zr(OETAP)_2]^+[SbCl_6]^-$ shows absorptions at 1096 and 1209 nm (maximum) with an inflection at 1280 nm. In contrast, $[Zr(OEP)_2]^+$ exhibits a maximum at 962 nm. It has been proposed

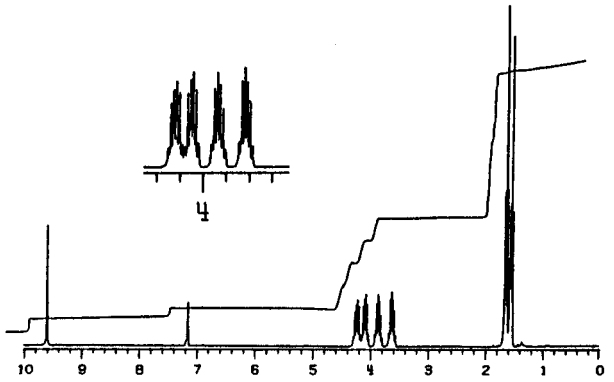

Figure 2. ^{1}H NMR spectrum of Zr(OEP)(OETAP) in C_6D_6.

that the energy of the near-IR band in these cation radicals indicates the strength of the $\pi-\pi$ interactions.[36−39] The above data are consistent with diminished interactions in $Zr(OETAP)_2$.

NMR. The ^{1}H NMR spectrum of Zr(OEP)(OETAP) in C_6D_6 is shown in Figure 2. All individual features of the porphyrins are clearly seen, including the two sets of well-resolved diastereotopic methylene signals. As was reported for the $Zr(OEP)_2$ sandwich,[2] the meso signal on the OEP subunit is shifted upfield relative to the monoporphyrin; however, the value of 9.60 ppm is a much smaller upfield shift than the 9.23 ppm in $Zr(OEP)_2$. The large upfield shift of all the signals in the sandwiches as compared to the monoporphyrins has been attributed to the effect of two ring currents.[5] Presumably this effect is diminished in the tetraazaporphyrin case.

IR. IR spectroscopy is a useful diagnostic in the characterization of porphyrin cation radicals. "Marker" bands, which are thought to arise from a strongly IR-allowed porphyrin ring mode and are diagnostic of a porphyrin radical cation, were initially used to determine whether oxidation in monoporphyrins occurred at the metal or the porphyrin π system.[40,41] The measurement of such "marker" bands has been extended to demonstrate the π radical character of the sandwich porphyrin cations. "Marker" bands in the region 1570−1535 cm^{-1} have been assigned to the π cation radical in OEP complexes.[41] For the $[Zr(OEP)_2]^+$ complex this band was observed at 1555 cm^{-1}.[2] In the case of mixed sandwiches, IR spectroscopy can be used to determine if the cation radical is isolated on one porphyrin or delocalized over both porphyrins. Since no characteristic "marker" band has been reported for the octaethyltetraazaporphyrin cation radical, the IR spectra of $[Zr(OETAP)_2]^+[SbCl_6]^-$ and $[Zn(OETAP)]^+[SbCl_6]^-$ were obtained and compared to the IR spectra of the corresponding neutral species. From these spectra it was possible to assign the $OETAP^+$ cation radical "marker" band as falling in the 1325−1310 cm^{-1} region. The spectrum of the monoporphyrin $[Zn(OETAP)]^+[SbCl_6]^-$ showed a band at 1311 cm^{-1} which was absent in Zn(OETAP) spectrum. Similarly, $[Zr(OETAP)_2]^+[SbCl_6]^-$ shows a "marker" band at 1321 cm^{-1}. For $[Zr(OEP)(OETAP)]^+[SbCl_6]^-$ a weak band appears at 1317 cm^{-1} in addition to a band at 1547 cm^{-1}, which corresponds to the OEP radical cation. Since "marker" bands corresponding to both OEP and OETAP are present in the mixed

(37) Donohoe, R. J.; Duchowski, J. K.; Bocian, D. F. *J. Am. Chem. Soc.* **1988**, *110*, 6119−6124.
(38) Perng, J.-H.; Duchowski, J. K.; Bocian, D. F. *J. Phys. Chem.* **1990**, *94*, 6684−6691.
(39) Duchowski, J. K.; Bocian, D. F. *J. Am. Chem. Soc.* **1990**, *112*, 3312−3318.
(40) Shimomura, E. T.; Phillippi, M. A.; Goff, H. M.; Scholz, W. F.; Reed, C. A. *J. Am. Chem. Soc.* **1981**, *103*, 6778−6780.
(41) Scholz, W. F.; Reed, C. A.; Lee, Y. J.; Scheidt, W. R.; Lang, G. *J. Am. Chem. Soc.* **1982**, *104*, 6791−6793.
(42) Kelly, S. L.; Kadish, K. M. *Inorg. Chem.* **1984**, *23*, 679−687.

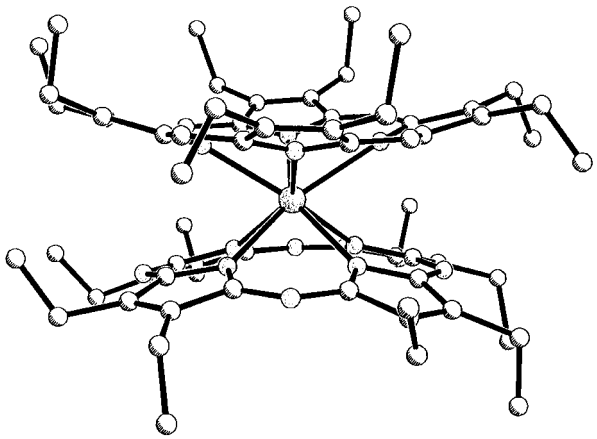

Figure 3. Perspective drawing of the solid-state structure of Zr(OEP)(OETAP). Carbon atoms are represented by medium-sized open spheres, the Zr atom is represented by a large shaded sphere, and the nitrogen atoms are represented by lightly-shaded medium-sized spheres.

complex, both ligands show π radical character, with the cation delocalized over both porphyrins in the mixed sandwich, indicating a strongly coupled π system.

EPR. The EPR spectra of $[Zr(OEP)(OETAP)]^+[SbCl_6]^-$ and $[Zr(OETAP)_2]^+[SbCl_6]^-$ were obtained as frozen 10^{-3} M CH_2Cl_2 solutions at 77 K. Both samples showed similar g values and line widths ($[Zr(OEP)(OETAP)]^+[SbCl_6]^-$, $g = 2.005$, line width = 2.4 G; $[Zr(OETAP)_2]^+[SbCl_6]^-$, $g = 2.005$, line width = 2.7 G) and confirmed the existence of an unpaired electron. No hyperfine structure was observed in either sample. The values were similar to the results obtained for $[Zr(OEP)_2]^+[SbCl_6]^-$.[2]

Cyclic Voltammetry. All of the sandwiches studied showed reversible electrochemical potentials by cyclic voltammetry. The data are compared in Table 2.

In THF, up to two reversible oxidations and up to three reversible reductions were observed within the solvent window. The first oxidation and first reduction of $Zr(OETAP)_2$ were each about 600 mV more positive than in $Zr(OEP)_2$. Under the same electrochemical conditions, the first oxidation of Zn(OETAP) was 400 mV more positive than Zn(OEP), and the first reduction was 628 mV more positive. Thus the OETAP oxidation potential is 200 mV more positive of OEP in the sandwiches than in the monoporphyrins. This difference would be expected if the $\pi-\pi$ bonding in the tetraazaporphyrins is weaker than in the porphyrins and the HOMO in the tetraazaporphyrin sandwich is less elevated in energy than in the porphyrin case. The electrochemical results are consistent with the near-IR data.

The first oxidation of the mixed porphyrin sandwich Zr(OEP)(OETAP) was slightly more positive than the average of the two homo-sandwich oxidations. Similarly, the first reduction was slightly more negative than the average of the two homo-sandwich reductions. These results have been observed before in mixed-sandwiches and are expected because the HOMO should contain more OEP character and the LUMO should have greater OETAP character on the basis of the relative redox potentials of the monoporphyrins.

Crystal Structures. The X-ray crystal structures of Zr(OEP)(OETAP) and $Zr(OETAP)_2$ were obtained from crystals grown by slow evaporation of saturated dichloromethane/acetonitrile solutions. An ORTEP plot of Zr(OEP)(OETAP) is shown in Figure 3, and selected metrical parameters are listed in Table 3.

The solid-state structures of the two sandwich complexes are similar to that reported for $Zr(OEP)_2$.[3] Two distinct porphyrin ligands are observed for each of the sandwich complexes as indicated by the two entries for Zr−Np[43] and $Zr-P_{24}$.[44] However, in the mixed sandwich the OEP subunit could not be distinguished from the OETAP subunit, and parameters for Zr(OEP)(OETAP) listed in Table 3 are averages of the corresponding homoporphyrins. Indistinguishability of the porphyrins in the mixed-sandwich indicates that the sandwiches are oriented randomly and the dipoles are not aligned in the crystal.

The distance from the zirconium to the mean plane of the coordinated nitrogens ($Zr-N_p$) is the same in OEP and OETAP. This similarity most likely occurs because the porphyrins are at the minimum separation allowed by steric interactions. The hole size (defined as the average distance between opposing coordinated pyrrole nitrogens) of the tetraazaporphyrin is smaller than that of the porphyrin, due to shorter bonds between the pyrrolic α-carbon and the bridging nitrogen atoms, as well as smaller bond angles between the bridging nitrogen atoms. A smaller hole size in the structure of Fe(OETAP)Cl was also observed by Fitzgerald.[26] The identical $Zn-N_p$ values and smaller OETAP hole size constrain the average bond length between the zirconium and the coordinated pyrrolic nitrogens ($Zr-N_{avg}$) to be shorter in the tetraazaporphyrin case.

Despite a smaller hole size in the tetraazaporphyrin, the zirconium is displaced from the mean plane of the coordinated nitrogens by the same distance as in OEP. The distance between the zirconium and the mean plane of the 24 atom core is slightly larger in the tetraazaporphyrin case, which leads to a slightly larger distortion of the OETAP core versus the OEP core and would be consistent with diminished porphyrin−porphyrin interactions in the former case. Finally, the porphyrins are twisted with respect to each other by similar amounts (43.8, 42.4, and 41.6° for $Zr(OEP)_2$, Zr(OEP)(OETAP), and $Zr(OETAP)_2$, respectively), indicative of similar steric parameters for OEP and OETAP. In contrast, the structure of $Zr(TPP)_2$ has a twist angle of 37°.[2]

EFISH Measurements. Electric field-induced second harmonic (EFISH) generation measurements were performed on Zr(OEP)(OETAP). The complex's Q′ band causes it to be slightly absorbent at the detection wavelength of 954 nm (Figure 2) which increases the uncertainty limits on the results. Nevertheless, it is clear that the hyperpolarizability β is negative. At 1907 nm, β was determined to be $(-83 \pm 43) \times 10^{-30}$ esu.

Extrapolation to zero frequency using the two-level model[45] yielded a value for β_0 of $(-62 \pm 32) \times 10^{-30}$ esu. The extrapolation is valid to the extent that only one of the complex's low-lying excited states contributes significantly to the hyperpolarizability. Promotion to this state must involve the largest amount of intramolecular charge transfer of any of the various excited states. For the purpose of this extrapolation, the Q″ band at 434 nm (in chloroform) was treated as the primary charge transfer excited state, based on state assignments for thorium porphyrin sandwich complexes.[36]

The dipole moment was determined in the same solvent using the Guggenheim analysis as previously described.[32] This analysis assumes that the solute has a substantially higher dipole moment than the solvent; in this case, the dipole difference was smaller than usual, again leading to large error bars. Chloroform has a dipole moment of 1.87 D; the mixed complex was found to have a dipole moment of 3.9 ± 2.0 D, which by obvious symmetry arguments is inferred to lie along the axis perpen-

(43) The symbol N_p is used to designate the center-of-gravity for the four coordinated pyrrole nitrogens of a porphyrin or azaporphyrin.
(44) The symbol P_{24} is used to designate the center-of-gravity of the 24 atom core of the coordinated macrocycle.
(45) Oudar, J. L.; Chemla, D. S. *J. Chem. Phys.* **1977**, *66*, 2664−2668.

Table 3. Selected Average Bond Lengths (Å), Angles (deg), and Metrical Parameters Involving Non-Hydrogen Atoms in Crystalline $Zr(OEP)_2$, Zr(OEP)(OETAP), and $Zr(OETAP)_2$[a,b]

param[b]	$Zr(OEP)_2$[c]	Zr(OEP)(OETAP)	$Zr(OETAP)_2$
$Zr-N_{av}$	2.383 (3, 5, 15, 8)	2.342 (3, 5, 9, 8)	2.308 (3, 5, 10, 8)
N−N (hole size)	4.040 (−, 10, 19, 4)	3.946 (5, 10, 20, 4)	3.859 (4, 9, 18, 4)
$Zr-N_p$	1.271, 1.260	1.260, 1.262	1.270, 1.269
$Zr-P_{24}$	1.578, 1.627	1.627, 1.619	1.646, 1.625
twist angle	43.8 (−, 6, 9, 4)	42.4 (4, 5, 6, 4)	41.6 (4, 4, 4, 4)

[a] Bond lengths and angles involving the metal atom and the porphyrin core have been averaged according to the idealized symmetry of the $Zr(Por)_2$ complex. The first number in parentheses following an average value of a bond length or angle is the root-mean-square estimated standard deviation of an individual datum. The second and third numbers, when given, are the average and maximum deviations from the averaged value, respectively. The fourth number represents the number of individual measurements which are included in the average value. [b] The symbols Zr-Np and $Zr-P_{24}$ are used to represent the centers-of-gravity for the four coordinated pyrrole nitrogens and the 24 atom core of the porphyrin macrocycle, respectively. N−N (hole size) is the average distance between opposing coordinated pyrrole nitrogens on the porphyrin. [c] Values are taken from ref 3.

dicular to the porphyrin rings, with the OETAP ring bearing the greater negative charge.

It has been shown that under the two-level model, the excited-state dipole moment may be determined[46] based on β, λ_{max}, the oscillator strength, and the ground-state dipole moment. For this mixed complex, the excited-state dipole moment is calculated to be −2.9 D, similar in magnitude but opposite in direction to the ground-state value. Clearly the two rings are coupled efficiently enough to permit substantial charge transfer through the metal ion upon excitation.

It is somewhat surprising that a complex like Zr(OEP)(OETAP) exhibits a hyperpolarizability as large as it does, given that a symmetric sandwich would have a β value rigorously equal to zero and that the asymmetry is small (donor and acceptor are both porphyrin rings). The conventional method of constructing nonlinear chromophores using porphyrins is to attach strong electron donors and acceptors to the opposite ends of the porphyrin macrocycle. This method causes intramolecular charge transfer to occur between the donor and acceptor substituents along the porphyrin plane and over a large distance. Indeed, Therien and co-workers have recently synthesized porphyrin complexes with substantial β values in exactly this manner.[47] The results on the mixed complex given here, however, suggest that the *z*-axis might be used effectively to generate complexes with nonlinearities as well. The advantage of *z*-axis polarization is that it does not require a large ground-state dipole moment, thereby allowing greater solubility in a variety of polymer matrices. One can, for example, imagine double-decker porphyrin sandwich complexes, with the ligands stacked in order of electronegativity. The dipole moment would be slightly larger due to the greater distance over which the charge is separated, and the achievable change in that dipole moment would be slightly larger for the same reason. The achievable change in that dipole might be 200% of the ground-state dipole, due to the reversal of direction like that observed with Zr(OEP)(OETAP). Since β is proportional to $\Delta\mu$, it may ultimately prove more efficient to design nonlinear chromophores whose excited-state dipole moments are equal to $-\mu g$ rather than $\mu g + x$.

Conclusion

A family of bis(porphyrin)zirconium(IV) sandwich complexes has been prepared in which the porphyrins differ dramatically electronically but only slightly sterically. The similar steric parameters of $Zr(OEP)_2$, Zr(OEP)(OETAP), and $Zr(OETAP)_2$ were established by X-ray crystallography. The difference in electronegativities of the ligands is magnified in the homo-sandwich oxidation potentials: $Zr(OETAP)_2$ is 600 mV harder to oxidize than $Zr(OEP)_2$ (*vs* a 400 mV difference in the monoporphyrins). Despite the large redox differences of the ligands, the one electron oxidized mixed-sandwich, $[Zr(OEP)(OETAP)]^+[SbCl_6]^-$, has an electron hole that is unsymmetrically delocalized over both porphyrins. The neutral mixed sandwich complex also exhibits delocalization over both porphyrin rings, as evidenced by reversal in dipole moment between the ground and Q″ excited states.

Acknowledgment. We thank Eric Enemark of the Department of Chemistry, Stanford University, and Dr. Fred Hollander of the College of Chemistry, University of California at Berkeley, for collecting X-ray data and Uma Sundaram of the Department of Chemistry, Stanford University, for assistance in EPR. We also thank the NSF (Grant CHE 9123187-A4) for financial support. The Mass Spectrometry Facility at the University of California at San Francisco is supported by NIH Division of Research Grant RR01614 and by NSF Grant DIR8700766.

Supporting Information Available: Tables listing detailed crystallographic data, atomic positional and thermal parameters, and bond lengths and angles and perspective structural drawings for Zr(OEP)(OETAP) and $Zr(OETAP)_2$ (42 pages). Ordering information is given on any current masthead page.

IC970657U

(46) Moylan, C. R.; Twieg, R. J.; Lee, V. Y.; Swanson, S. A.; Betterton, K. M.; Miller, R. D. *J. Am. Chem. Soc.* **1993**, *115*, 12599−12600.
(47) LeCours, S. M.; Guan, H.-W.; DiMagno, S. G.; Wang, C. H.; Therien, M. J. *J. Am. Chem. Soc.* **1996**, *118*, 1497−1503.